Green Chemistry

ARTICLE TYPE

Recyclable hydrotalcite catalysts for alcohol imination via acceptorless dehydrogenation

**John Bain[a], Philip Cho[a], Adelina Voutchkova-Kostal[*a]**

Here we report that hydrotalcite-like materials (HTs) are active heterogeneous catalysts for alcohol imination, which proceeds through acceptorless alcohol dehydrogenation. Catalytic activity of a series of Mg-Al hydrotalcites doped with Fe^{3+}, Zn^{2+}, Ni^{2+}, Cr^{3+} and Cu^{2+} is dependent on their composition, and Fe:Mg:Al HT yields up to 92% imine under mild conditions. Impregnation of Fe:Mg:Al HT with Pd^0
10 resulted in enhancement of activity for acceptorless dehydrogenation, but a decrease in the isolated yield of imine in a loading-dependent manner. This is attributed to the Pd loading-dependent retention of imine and aldehyde on the catalysts. The substrate scope for alcohol imination and recyclability of the catalysts are discussed.

Introduction

15 Imines are highly versatile intermediates for the stereoselective synthesis of amines and *N*-heterocycles.[1] Synthetic routes to imines that utilize readily available starting materials, such as alcohols, are typically more atom economical than conventional routes requiring carbonyl compounds. Alcohol imination
20 reactions can proceed through alcohol oxidation to the corresponding ketone or aldehyde, followed by condensation with the amine. Amination catalysts typically proceed through alcohol dehydrogenation, amine condensation and imine hydrogenation (Scheme 1a).[2-10] Alcohol imination can proceed through a similar
25 route lacking the hydrogenation step (Scheme 1b). Although a number of highly active catalysts have been reported for alcohol amination,[4, 8, 10-18] catalytic systems that yield the imine are rare, and offer the advantageous possibility of further imine functionalization.[17, 19-23]

(a)
(b)
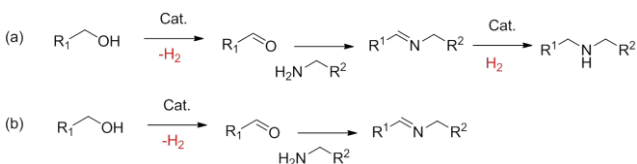
30 **Scheme 1** (a) Catalytic alcohol (a) amination and (b) imination via dehydrogenation.

Hydrotalcites (HTs) are layered double hydroxides (LDHs)[24] with general formula of $[M^{2+}_{1-x}M^{3+}_{x}(OH)_2]^{x+}(A^{n-})_{x/n}\cdot mH_2O$, where A^- represents anions (e.g. CO_3^{2-}, OH^-, Cl^-, NO_3^{2-}, SO_4^{2-} *etc.*) and
35 M^{2+} and M^{3+} are compatible alkali earth and transition metal ions, (e.g. Fe^{3+}, Zn^{2+}, Ni^{2+}, Cr^{3+}, Cu^{2+}, Co^{2+}, *etc*). Although variation in the composition does not impact the brucite-like structure,[24] it does affect the acid/base,[25-28] redox,[28, 29] and catalytic properties of these materials.[25, 30-34] Particle size and morphology can also
40 be varied by modifying the synthetic protocol.[35-38] In addition, the

LDH structure itself can be semi-reversibly transformed to that of a mixed metal oxide (MMO) by calcination at ~450°C.[39, 40] MMOs outperform the corresponding LDHs in a number catalytic applications, as they are significantly more basic and resistant to
45 sintering.[39] Rehydration of MMOs causes incomplete reversion to a more basic LDH phase via a "memory effect".[34, 41] Thus, by controlling composition, synthetic protocol and post-synthetic treatment a palette of synthetic HTs can be accessed with comparable structures, but substantial differences in catalytic
50 activities. This allows optimization of the catalytic activity by varying HTs composition.[39]

HTs are increasingly used as heterogeneous catalysts for a number of base-assisted solution-phase reactions that operate under mild conditions. Examples include Aldol condensations,[42-
55 44] Claisen-Schmidt condensations,[45] acylation of phenols, amines and thiols,[46] epoxidations,[47] transesterifications,[48] and *N*-arylation of amines.[49] HTs have also been reported as catalysts for alcohol oxidation that takes place under mild conditions: Sakthive *et al* have recently reported a Co/Al hydrotalcite system;[50] and
60 Choudary[51] and Takehira[52] have reported a Ni/Mg/Al hydrotalcite system for alcohol oxidation using molecular oxygen. However, acceptorless alcohol dehydrogenation is a more attractive approach due to the higher atom economy and generation of hydrogen gas. The catalytic activity of Mg-Al HTs for
65 acceptorless alcohol dehydrogenation is only reported under high temperature and pressure conditions (533K, 100 kPa) in the gas phase.[53] Alcohol imination using HTs has not been reported to the best of our knowledge, but there is one example of alcohol amination using a Cu/Al hydrotalcite, which likely proceeds
70 through alcohol dehydrogenation.[54]

In addition to the interest in HTs as heterogeneous catalysts, they are also increasingly used as "inert" supports for other catalysts. Examples include supported Rh,[55] V,[56] and Ru[57] oxides

and nanoparticles (n.p.) of Ag,[58] Pd,[59] Au,[60] Cu,[61] Ru,[62] Rh,[63] and Ni[64]. Nanoparticles of Ag, Pd, and Cu supported on Mg-Al HTs are reported as active catalysts for acceptorless alcohol dehydrogenation under mild conditions. Although these reports
5 note that the HT support is critical for catalytic activity, [61, 62, 65-68] they do not attribute inherent catalytic activity for dehydrogenation to the HT itself.[52, 62, 69, 70]

While exploring the catalytic activity of HT-supported Pd n.p. for alcohol imination, we observed that some HTs exhibit
10 inherent catalytic activity for alcohol dehydrogenation and imination. Here we report the optimization of a modified hydrotalcite that can act as an efficient, cheap and recyclable heterogeneous catalysts for alcohol imination under mild conditions. We show that supported Pd[0] can enhance activity for
15 dehydrogenation, but actually retard activity for imination.

Results and discussion

Six modified Mg-Al hydrotalcites (HTs) were synthesized with the addition of first row transition metal ions. First row metals
20 were selected due to their relative abundance in comparison to second and third row transition metals, and the compatibility of their ionic radii for incorporation into the HT lattice. The metal ions selected (Cr^{3+}, Fe^{3+}, Ni^{2+}, Cu^{2+} and Zn^{2+}) provide a range of acid-base properties, hydridic/protic behaviour and redox
25 potentials. HTs *1-6* were synthesized by co-precipitation and aging of the corresponding transition metal nitrate salt with $Mg(NO_3)_2.6H_2O$ and $Al(NO_3)_3.9H_2O$. Table 1 shows the elemental composition, powder x-ray diffraction (PXRD) parameters and BET surface areas of the resulting HTs *1-6*. The
30 PXRD and BET surface area parameters are consistent with literature values (ESI Table-S1).

Table 1 Characterization data of hydrotalcites (HTs) *1-6*.

Cat.	M[a]	% Elemental composition (FAAS)			PXRD crystallographic parameters[b]			BET S.A. (m²/g)
		Mg	Al	M[a]	a (Å)	c (Å)	L (nm)	
HT*1*	-	28.3	9.28	-	3.001	23.348	16.9	63
HT*2*	Zn	20.9	6.95	29.0	3.005	23.186	10.0	128
HT*3*	Cu	21.9	8.54	13.2	2.992	22.986	15.0	30
HT*4*	Fe	29.4	3.05	11.4	3.082	23.145	20.0	73
HT*5*	Ni	25.0	10.2	14.0[c]	2.998	23.346	12.9	64
HT*6*	Cr	25.2	3.36	10.1[c]	3.020	23.067	11.9	5

[a] Third metal added to the Mg/Al HT; [b] *a*, the average cation-cation
35 distance; *c*, three times the distance from the centre of one brucite-like layer to the next layer; *L*, the average crystallite size (lower bound, calculated using Scherrer's formula);[71] [c] Values obtained by EDX.


Powder X-ray Diffraction (PXRD) patterns confirmed the
40 phase, phase transition, crystallinity and lattice parameters of the HTs, as well as Pd-impregnated HTs (Pd/HTs) discussed in a later part of the manuscript. Exemplary PXRD patterns are shown in Figure 1. The PXRD patterns of all six HTs (shown in ESI-Figure S1) were consistent with pure HT phase, characterized by
45 sharp symmetric reflections (*003* and *006*) and broad asymmetric

reflections.[24] The lattice parameters *a* and *c* (average cation-cation distance and three times the distance from the centre of one brucite-like layer to the next, respectively) were all within 0.015 Å and 0.92 Å ranges respectively, suggesting only minute
50 differences in the lattice structures of the HTs. The variation in composition is reflected in an evident variability in the BET surface areas of HT*1-6* (5-128 m²/g). This is due to small differences in the synthetic protocols for the respective HTs, differences in the rates of co-precipitation and porosity of the
55 resulting HT. The BET surface area of the HT*6*, which contains 10.1% Cr^{3+}, is reproducible but anomalously low due to very low porosity relative to the other HTs. PXRD and FT-IR characterizations of HT*6* were consistent with HT as the only phase.
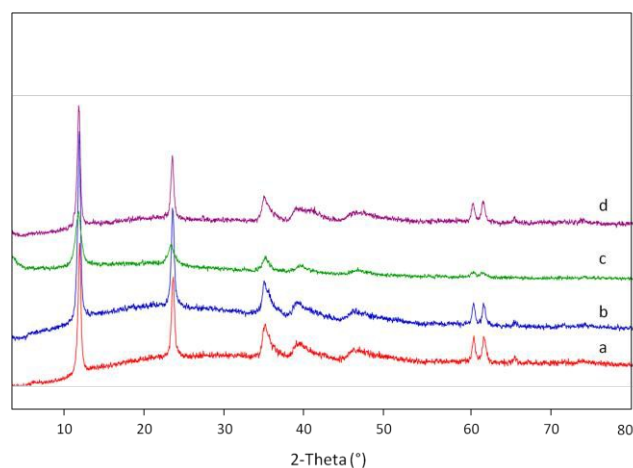
60 **Fig.1** PXRD patterns of (a) HT*4*, (b) 0.02% Pd/HT*4*, (c) 1% Pd/HT*4*, and (d) 5% Pd/HT*4*

HTs *1-6* were also characterized by FT-IR. Figure 2 shows exemplary FT-IR spectra of HT*4* and the series of Pd/HT*4* with
65 varying loadings of Pd, while spectra for HT*1-6* are shown in ESI-Figures S2. Carbonate anions were detected in all HTs and Pd/HTs, as indicated by the $\nu_{C=O}$ at 1350-1370cm⁻¹. Broad bands arising from bending vibrations of interlayer water are observed between ~1400 and 1700 cm⁻¹. Since the symmetry of the
70 interlayer water molecules is affected by composition, some HTs show additional broad bands in that region. Nitrate anions were not detected (no sharp peak at 1376 cm⁻¹),[72] indicating nitrate salts of the starting materials had been washed out of the lattice.
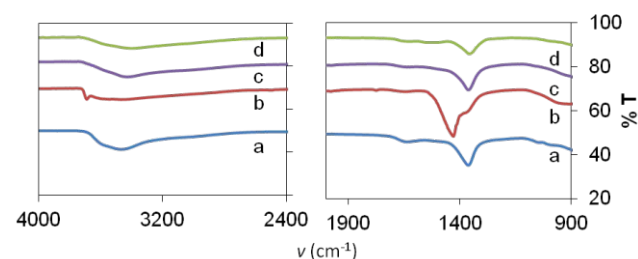
75 **Fig. 2** FT-IR spectra of (a) HT*4*, (b) 0.02% Pd/HT*4*, (c) 1% Pd/HT*4*, and (d) 5% Pd/HT*4*

Catalytic activity of hydrotalcites for alcohol dehydrogenation and imination

The catalytic activity of HT*1-6* towards alcohol dehydrogenation

(Scheme 2) and imination (Scheme 3) of benzyl alcohol in the absence of a base is summarized in Figure 3. The yields of aldehyde resulting from alcohol dehydrogenation are lower than the yields of imine, which implies that the amine improves dehydrogenation yield by drawing the equilibrium towards products via condensation with the aldehyde. A general correlation between the activity for both reactions was observed, consistent with imination occurring via dehydrogenation. The mole ratio of H_2 to benzaldehyde was within experimental error of being stoichiometric (89:100) in the dehydrogenation of benzyl alcohol, thus indicating H_2 is generated quantitatively during the reaction. A clear difference in catalytic activity was observed among the six HTs. In contrast to the negligible yield of the imine afforded by HT**6** (Cr:Mg:Al), HT**4** (Fe:Mg:Al) afforded 85% imination product under the screening conditions. The observed relative catalytic activity of the HTs for imination is as follows:

Fe:Mg:Al (HT**4**) > Ni:Mg:Al (HT**5**) > Mg:Al (HT**1**) > Cu:Mg:Al (HT**3**) > Zn:Mg:Al (HT**2**) >> Cr:Mg:Al (HT**6**)

Optimization of solvent for imination reactions increased the yield afforded by HT**4** to 92% when xylenes was used as solvent. The reaction proceeds without the need for an external base, and addition of K_2CO_3 did not improve the yield. Although the aniline present is itself a homogeneous base, results from alcohol dehydrogenation experiments confirm that no external base is necessary for dehydrogenation. In contrast, homogenous catalysts for similar processes do not generally operate efficiently without an external base.[17]
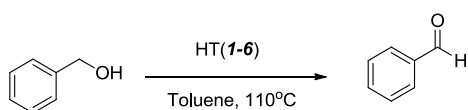
Scheme 2. Catalyst screening for alcohol dehydrogenation.
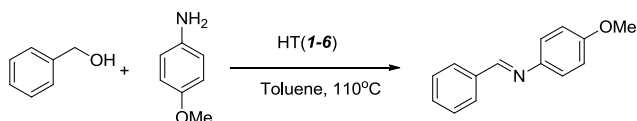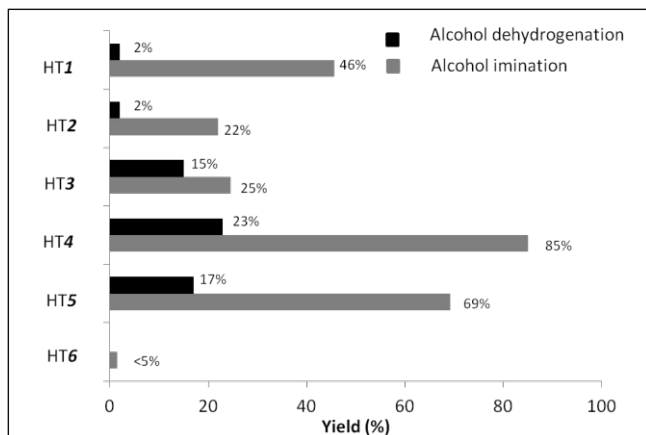

Scheme 3. Catalyst screening for alcohol imination.

Fig.3 Percent yields of benzaldehyde and 4-methoxy-*N*-(phenylmethylene)benzenamine from reactions in Scheme 2 and 3. Alcohol dehydrogenation reaction conditions: 0.24 mmol of benzylalcohol, 0.100 g of catalyst, 3 mL toluene, 110°C, 48 hrs. Yields were determined from GC-FID with an internal standard

(trimethoxybenzene). Alcohol iminations were carried out under identical conditions, with the addition of 0.29 mmol p-anisidine.

Given that the similar lattice structures of the six HTs, these differences in activity are likely due to respective acid-base properties, redox properties, and catalytic surface areas. Although differences in surface areas cannot account for the variation in catalytic activity, the lack of activity for HT**6** is likely associated with its anomalously low surface area and the lack of porosity, that is apparent from the gas adsorption isotherms. The differences in acid-base and redox properties are currently under investigation, and likely have the predominant influence on catalytic activity. Preliminary microcalorimetry results[78] that probe the heats of adsorption of CO_2 found HT**4** to have intermediate basicity among the series, which implies that there is likely an optimal basicity associated with highest catalytic activity. It should also be noted that trends from microcalorimetric studies are impacted by surface area, volume of pore or diameter of pore. The latter three are not consistent across HT **1-6**, as indicated in Table 1, so further research efforts are focused on optimizing the synthetic protocols so as to make surface areas consistent. This will allow us to explicitly probe the effect of basicity.

Since the basicity of HTs can be enhanced semi-reversibly by calcination[39, 40] and by calcination-rehydration[34, 41] we also probed the catalytic activity after calcination of HT**4** at 450 °C and after calcination-rehydration. This treatment afforded HT**4**$_{calc}$ and HT**4**$_{reh}$ respectively. Under optimised conditions both were less active for imination than the HT**4**, although HT**4**$_{calc}$ showed higher dehydrogenation activity.(Table 2).

Table 2. Percent yields of (a) 4-methoxy-*N*-(phenylmethylene) benzenamine and (b) benzaldehyde from imination or dehydrogenation of benzyl alcohol facilitated by HT**4** with different thermal treatment (HT**4**: freshly prepared; HT**4**$_{calc}$: calcined at 450 °C and HT**4**$_{reh}$: calcined at 450 °C then rehydrated).

	HT**4**	HT**4**$_{calc}$	HT**4**$_{reh}$
Dehydrogenation (*Sch. 2*)^a	23	37	8
Imination (*Sch. 3*)^a	92	77	38

^{a,b}Conditions as described in Figure 3.

We initially hypothesized that the enhanced basicity of HT**4**$_{calc}$ and HT**4**$_{reh}$ would translate into higher activity for dehydrogenation, as the basic sites are implicated in deprotonation of the alcohol and β-hydride elimination. Indeed we observe a higher dehydrogenation yield with HT**4**$_{calc}$. However, HT**4**$_{calc}$ and HT**4**$_{reh}$ both afford lower imination yields than HT**4**. To test whether this decrease in yield is due to the adsorption of aldehyde and/or imine to the HT, we monitored the concentration of free aldehyde and imine respectively when each was reacted with HT**4**, HT**4**$_{calc}$ and HT**4**$_{reh}$ respectively. We found that HT**4**$_{calc}$ retains 53% and 41% after 24h of reaction. Under the same conditions HT**4**$_{reh}$ retains 28% of the imine and 35% of the aldehyde respectively. Given that HT**4** retains smaller fractions of aldehyde and imine, the lower yields of aldehyde (for HT**4**$_{reh}$) and imine (for HT**4**$_{calc}$ and HT**4**$_{reh}$) are likely due to the adsorption of the products on the catalyst. Extensive washing of the catalyst did

not release additional products.

Catalytic activity of Pd[0] on Fe-Mg-Al hydrotalcite for alcohol dehydrogenation and imination

Given that HT*4* was the most active HT catalyst for both dehydrogenation and imination, we expected that immobilization of small quantities of Pd(0) on this support would boost catalytic activity. This is consistent with literature reports that document alcohol dehydrogenation facilitated by immobilized Pd on Mg/Al HT.[62, 65, 73] We thus synthesized and characterized three Pd/HT*4* catalysts with different Pd loadings (Table 3). The presence of Pd was confirmed by AAS and TEM/EDX. TEM images did not show distinct Pd nanoparticles, suggesting the Pd phase is highly dispersed (ESI-Figure S3). The PXRD parameters and the elemental composition of palladium on HT*4* are shown in Table 3. PXRD patterns showed no detectable Pd phase and only minor variations from the crystallographic parameters of HT*4* (Figure 1). No detectable change in the HT*4* interlayer spacing by PXRD is consistent with a highly dispersed Pd phase.[74, 75] The FT-IR spectra of Pd/HT*4* show broadening of the O-H (ν_{O-H} at 3000-3600 cm^{-1}) bands, suggesting a greater degree of hydrogen bonding in the surface and/or interlayer water. Small shifts in the carbonate band ($\nu_{C=O}$ at ~1400 cm^{-1}) and stretches related to interlayer water at 1560-1700 cm^{-1} likely result from the changes in the symmetry of interlayer water molecules.

Table 3. Characterization data of Pd/HT*4* catalysts (Pd/HT*4*): Pd composition (determined from Atomic Absorption Spectroscopy) and PXRD crystallographic parameters (*a, c and L*).

Catalyst	% Pd (AAS)	PXRD crystallographic parameters [a]		
		a (Å)	*c* (Å)	*L* (nm)
0.02% Pd/HT*4*	0.020	3.097	23.640	16.9
1% Pd/HT*4*	1.050	3.052	22.711	12.6
5% Pd/HT*4*	4.875	3.055	23.226	12.0

[a] *a*, the average cation-cation distance; *c*, three times the distance from the center of one brucite-like layer to the next layer; *L*, the average crystallite size (lower bound, calculated using Scherrer's formula).[71]

The catalytic activity of the Pd/HT*4* as it relates to the Pd loading is illustrated in Figure 4 and Table 4.
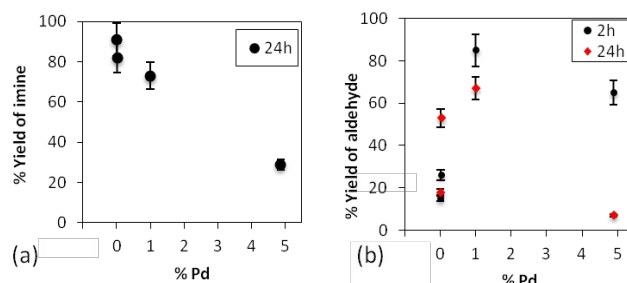
Table 4. Percent yields of benzaldehyde and 4-methoxy-*N*-(phenylmethylene) benzenamine from reactions in Scheme 2 and 3.

Catalyst	mol %Pd[a]	%Yield		
		Imine, 24h[b]	Aldehyde, 2h[c]	Aldehyde, 24h[c]
HT*4*	0	92	15	23
0.02% Pd/HT*4*	0.001	82	26	53
1% Pd/HT*4*	0.039	73	85	67
5% Pd/HT*4*	0.191	29	65	7

[a] mol% Pd relative to benzyl alcohol [b,c] Conditions as described in Figure 3.

The aldehyde yields isolated from alcohol dehydrogenation (Scheme 2) were dependent on the Pd[0] loading, with the highest

yield (85%) obtained with the 1% Pd/HT*4* catalyst after 2h (0.039 mol% Pd vs alcohol), dropping to 65% when Pd[0] loading on HT*4* was increased to ~5% (0.191mol% Pd). The trend is illustrated in Figure 4. The lower yields with 5% Pd/HT*4* are likely due to the agglomeration of Pd, as confirmed by TEM. In comparison, in the 1% Pd/HT*4* catalyst no distinct nanoparticles were observed by TEM, suggesting a more disperse Pd phase. The fact that Pd impregnation enhances the aldehyde yield suggests that HT*4*-supported Pd[0] is more catalytically active for dehydrogenation than the support (HT*4*) alone. Interestingly, the aldehyde yields were higher at 2h of reaction than at 24h (Table 4). The decrease was especially noticeable for reactions with 5% Pd/HT*4*, where the aldehyde yield decreased from 65% (2h) to 7% (24h). Since the recovered unreacted alcohol can account for mass balance, we hypothesized that this was due to aldehyde being adsorbed to the catalyst. Thus we quantitated the fraction of free aldehyde in control reactions, where the alcohol was replaced by aldehyde under identical reaction conditions. We found that while the loss of aldehyde with 0.02% Pd/HT*4* is negligible, with 1% Pd/HT*4* we lose up to 30% of the aldehyde in 2 hr, while with the 5% Pd/HT*4* that number increases to 44%, and these quantities increase with time. These results suggest that the lower yield of aldehyde after 24h vs after 2h could be attributed to adsorption of the aldehyde to Pd/HT*4*. The quantity of aldehyde bound is dependent on the loading of Pd on the HT (and the mol% Pd).

Fig. 4 Percent yields of (a) imine from Scheme 3 and (b) benzaldehyde from Scheme 2 versus % Pd loading on HT*4*. Reaction conditions: 0.24 mmol of benzylalcohol, mol % Pd as shown in Table 4, 3 mL toluene, 110 °C, 24 hrs). Yields were determined from GC-FID using trimethoxybenzene as an internal standard. Error bars designate estimated standard error arising from measurement error and multiple runs.

The yield of imine from the reaction in Scheme 3 decreases almost linearly with increasing Pd loading (Table 4 and Figure 4). Thus, HT*4* is the most active catalyst (91% yield), but just 0.02% Pd loading on the catalyst (0.001mol% Pd) causes a decrease in the isolated yield to 82%. We proposed that this trend is due to the retention aldehyde, amine and/or imine by the catalyst, and this retention is dependent on the Pd loading. Free aniline was observed in the reactions and accounted for by mass balance, and a Pd loading-dependent retention of aldehyde was already established in the previously described experiment. The amount of imine retained was about equal for HT*4* and 1%Pd/HT*4* (22-26%) but higher for 5%Pd/HT*4* (43%). Strong binding of Pd to imines is not surprising given the homogeneous catalysis literature. Despite the fact that these results are consistent with the hypothesis, we have not excluded the possibility that there may be more complex reasons that drive the difference in imine yields obtained from Pd/HT*4* catalysts and HT*4*, such as the

effect of immobilized Pd on the number and strength of acid-base sites on the HT*4*. Microcalorimetric studies are underway to investigate the effect of Pd on the acid-base properties of HTs. Although we typically report TON and TOF when describing a new catalyst, in this case these metrics cannot be meaningfully established as the active sites on these catalysts have not yet been identified or quantified. That is to say, we cannot assume that the Pd species are the only active catalyst, as our data clearly shows the HT*4* itself is catalytically active for alcohol dehydrogenation. The investigation of the mechanism and active sites of these catalysts are the topic of ongoing investigation, and include an in-depth study of the electronic support interactions between Pd and HT*4*.[40, 76]

Substrate Scope for Imination

The alcohol substrate scope for imination using HT*4* under optimized reaction conditions is shown in Table 5. Benzylic alcohols generally showed good to excellent yields. The reaction is favoured by electron-donating substituents of the benzene ring, such as methoxy (entries 1,3: 97%, 89%), and disfavoured by strongly electron-withdrawing nitro groups, which reduce the yield to 75% (entry 5). Benzyl alcohol itself also gave excellent yields of imine (90%, entry 2). Interestingly, a low yield was obtained with 4-(hydroxymethyl)phenol (15%, entry 7) despite the electron-donating -OH group. Phenol could be deprotonated by the basic catalyst to form the corresponding phenoxide, which could competitively inhibit activation of the benzylic alcohol on the HT*4*. The resulting phenoxide might also intercalate and become immobilized in the HT interlayers, resulting in decreased product yield. The extension of the benzylic alcohol by one methylene group to phenethyl alcohol reduces the yield to 32%, indicating that this mild catalytic system is selective for activated alcohols. Primary and secondary aliphatic alcohols show no reaction under these conditions (entries 8 and 9). It is notable that under conditions reported by Uemura et al, Pd/HT systems do not show similar selectivity for alcohol dehydrogenation,[69, 70, 77] and are reactive for aliphatic alcohols.

The amine substrate scope using optimized reaction conditions and HT*4* is shown in Table 6. The yields observed with anilines were strongly influenced by the ring substituents. Anilines with electron donating groups, such as methoxy (entry 1), afforded high yields, while those with strongly electron-withdrawing nitro group resulted in lower isolated yields (entry 2). These electronic effects of ring substitution mirror the trends observed in the alcohol substrate series and are reflective of the more nucleophilic anilines being more reactive. The yields obtained with primary aliphatic amines were reasonably good (43-57%, entries 3, 4, 5). The results are not reflective of a direct trend with amine basicity, likely because more basic amines adsorb on the HT more strongly and are not available to condense with the aldehydes.

Catalyst Recycling

The ability to reuse the heterogeneous catalyst and identify compositional and morphological changes post-catalysis is critical for synthetic applications. Since in a few instances we observed conversions that were greater than yields, it was prudent to characterize the used catalysts, ensure organic material is not retained and check whether activity is retained in multiple use cycles. Indeed TGA of the used and unwashed catalyst (HT*4*) from reaction in Entry 1 in Table 5 showed a new mass loss at 185 °C. We find that aqueous potassium carbonate provides the necessary abundance of carbonate ions to reform the active catalyst quickly during the wash and remove adsorbed substrates. The reformation to a LDH phase was confirmed by FT-IR and PXRD (Figure 6), while the loss of residual organics was confirmed by TGA. The PXRD pattern of the used catalyst prior

Table 5 Alcohol substrate scope for HT*4*-catalyzed alcohol imination.

Entry	Alcohol substrate	Product	Yield %
1[a]			97
2[a]			92
3[a]			89
4[a]			84
5[a]			75
6[a]			32
7[a,b]			15
8[b]		-	NR
9[b]		-	NR

Reaction Conditions: [a]0.24 mmol alcohol, 0.60 mmol p-anisidine, 100 mg catalyst, 3 mL xylenes, 110 °C, 24hr. [b] 200 mg catalyst

to wash shows new reflections at 8.23° and 31.5° (2θ), which could not be readily attributed to an identifiable phase, but disappeared after aqueous K_2CO_3 wash. It is notable that the

PXRD patterns of the unwashed catalyst do not show any shift of the *003* reflection, which indicates there is no change in interlayer spacing that would likely result from intercalation of substrates or products. The FT-IR spectra were consistent with the PXRD data − the unwashed catalyst shows several new IR stretches in the hydroxyl and carbonyl regions that are eliminated after the aqueous K_2CO_3 wash. The PXRD patterns and FT-IR spectra of the washed catalyst closely resemble that of the fresh.

Table 6 Amine substrate scope for HT*4*-catalyzed alcohol imination.

Entry	Amine Substrate	Product	Yield %
1[a]	MeO—⟨⟩—NH₂		97
2[a]	O₂N—⟨⟩—NH₂		20
3[a]			43
4[a]			57
5[b]			57

Reaction Contions: [a]0.24 mmol benzyl alcohol, 0.29 mmol amine, 100 mg catalyst, 3 mL xylenes, 110 °C, 24hr. [b]0.6 mmol amine.

Given these results, it was thus not surprising that as long as an aqueous K_2CO_3 wash is performed, the catalyst retains its activity for at least 3 cycles with minimal loss in activity (Figure 5). In contrast, the unwashed catalyst shows loss of catalytic activity quickly over 3 cycles (Figure 5).
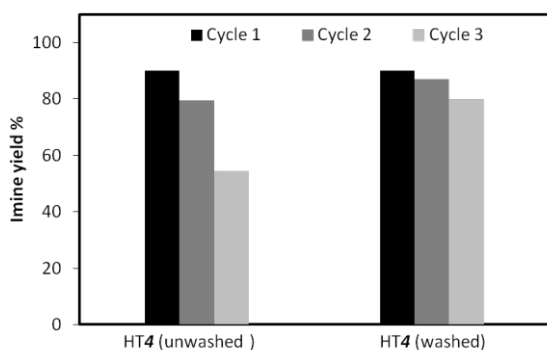
Fig. 5 Percent yields of 4-methoxy-*N*-(phenylmethylene)benzenamine from repeated cycles of the alcohol imination reaction between benzyl alcohol and *p*-anisidine catalyzed by HT*4*.

Conclusions

We developed an active hydrotalcite-like (HT) heterogeneous catalyst for alcohol imination proceeding through acceptorless alcohol dehydrogenation. After screening HTs with variable composition (up to 15% of Fe^{3+}, Zn^{2+}, Ni^{2+}, Cr^{3+} or Cu^{2+}), we identified Fe:Mg:Al HT (HT*4*) as the most active for both dehydrogenation and imination. The yields of imine generally exceeded those of aldehydes, suggesting that the amine drives the equilibrium forward by condensation. Calcination slightly increased the activity for dehydrogenation but significantly lowered
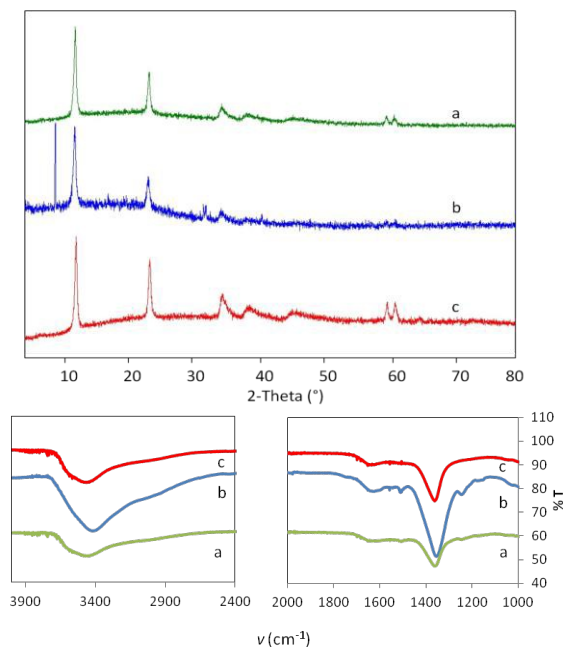
Fig. 6 Powder X-ray diffraction patterns (above) and FT-IR spectra (below) of (a) HT*4* washed with $K_2CO_3(aq)$ after imination reaction, (b) HT*4*-used and unwashed and (c) fresh HT*4*.
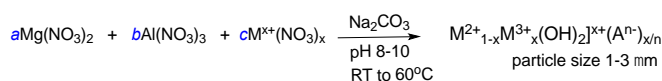
activity for imination. Thus, we opted to enhance the catalytic activity of non-calcined HT*4* by impregnating with Pd^0 at 0.02%, ~1% and ~5% loading. The dehydrogenation activity of the catalysts was enhanced by Pd(0) immobilization, with 1% Pd/HT*4* affording the highest yield of aldehyde. However, the imination activity was reduced in a loading-dependent manner. Our experiments suggest the primary reason for this was the Pd loading-dependent retention of aldehyde and imine on the catalysts. Substrate scope investigations revealed the catalytic system is selective towards activated alcohols and aromatic amines. Recyclability experiments showed that the catalytic activity for imination can be retained for at least three cycles when HT*4* is washed in aqueous K_2CO_3.

Experimental

Synthesis of HTs

Magnesium-alumnium hydrotalcites containing 0-15% Fe^{3+}, Zn^{2+}, Ni^{2+}, Cr^{3+}, Cu^{2+} were synthesized by aqueous co-precipitation of M^{2+} and M^{3+} nitrate salts under basic conditions (pH 8-10) in the presence of sodium carbonate (See Scheme 4 and ESI for details).[24, 58] The precipitates were filtered and washed copiously with deionized water until no more nitrate was present in the

filtrate. The resulting hydrotalcites were dried at 110 °C for 12 hours, and a fraction of each sample was calcined at 450 °C for 24 hrs.

$$a\,Mg(NO_3)_2 \;+\; b\,Al(NO_3)_3 \;+\; c\,M^{x+}(NO_3)_x \xrightarrow[\substack{pH\ 8\text{-}10 \\ RT\ to\ 60^oC}]{Na_2CO_3} M^{2+}{}_{1-x}M^{3+}{}_x(OH)_2]^{x+}(A^{n-})_{x/n,} \quad particle\ size\ 1\text{-}3\ mm$$

Scheme 4. Co-precipitation synthesis of hydrotalcites

Pd⁰ supported on hydrotalcites

A series of Pd⁰/HT**4** catalysts were prepared by wet precipitation-reduction. In a typical reaction, 2.00 g of calcined HT was suspended in deionized water (50 mL). To this suspension a known quantity of PdCl₂ was added, followed by the addition of 1 mL of a 1 M NaOH solution. The solution was allowed to stir at room temperature for 12 hours, after which the solution is removed via vacuum filtration, and the solid is washed with deionized water (3x 25mL) and dried for 12 hours at 110 °C. The solid was then resuspended in deionized water (50 mL) and reduced by dropwise addition of a NaBH₄ solution (0.01 g, 3 equivalents dissolved in 25 mL distilled water). The suspension was allowed to stir at room temperature for 2 hours, and then the solid was filtered and washed with deionized water (3 x 15 mL) and dried for 12 hours at 100 °C. Catalyst characterization is described in the ESI.

Alcohol dehydrogenation reactions

In a typical procedure, a 20 mL reaction tube was charged with 0.100 g of catalyst (or other amount, as indicated). It was then evacuated and placed under a nitrogen atmosphere. Subsequently, the alcohol (0.24 mmol, 1 eqiv) and 3 mL of degassed solvent were added to the reaction tube. The reaction mixture was heated to 110 °C for 24 hours in a Heidolph Radleys Carousel 12 Plus Reaction Station. The reaction was filtered and the spent catalyst was washed with toluene (3 x 5 mL) and K₂CO₃(aq) (3 x 5 mL). The filtrate was dried *in vacuo*, and the product was isolated by column chromatography using 80:20 hexanes/ethyl acetate. The isolated product was characterized by GC-MS, GC-FID and ¹H NMR.

Alcohol imination reactions

In a typical procedure, a 20 mL reaction tube was charged with 0.100 g of catalyst (or other amount, as indicated), then evacuated and placed under a nitrogen atmosphere. Subsequently the alcohol (0.24 mmol, 1 eqiv), amine (0.29 mmol, 1.2 equiv) and 3 mL of degassed solvent were added. The reaction mixture was heated to 110 °C for 24 hours in a Heidolph Radleys Carousel 12 Plus Reaction Station. The reaction was filtered and the spent catalyst was washed with toluene (3 x 5 mL) and K₂CO₃(aq) (3 x 5 mL). The filtrate was dried *in vacuo*, and the product was isolated by column chromatography. The product was characterized by GC-MS and ¹H NMR.

Acknowledgements

Notes and references

a Department of Chemistry, The George Washington University Washington, DC; Fax: 202-994-5873; Tel: 202-994-6121; E-mail: avoutchkova@email.gwu.edu

1. S. I. Murahashi, *Angewandte Chemie-International Edition in English*, 1995, **34**, 2443-2465.
2. M. A. Berliner, S. P. A. Dubant, T. Makowski, K. Ng, B. Sitter, C. Wager and Y. S. Zhang, *Org Process Res Dev*, 2011, **15**, 1052-1062.
3. J. F. Moulder, W. F. Stickel, P. E. Sobol and K. D. Bomben, *Handbook of X-ray Photoelectron Spectroscopy*, Physical-Electronics Inc., **Eden Prairie, MN** 1995.
4. R. Kawahara, K. Fujita and R. Yamaguchi, *Adv Synth Catal*, 2011, **353**, 1161-1168.
5. R. Yamaguchi, S. Kawagoe, C. Asai and K. I. Fujita, *Organic Letters*, 2008, **10**, 181-184.
6. K. Fujita, Z. Z. Li, N. Ozeki and R. Yamaguchi, *Tetrahedron Lett*, 2003, **44**, 2687-2690.
7. M. Benitez, E. Mas-Marza, J. A. Mata and E. Peris, *Chem-Eur J*, 2011, **17**, 10453-10461.
8. G. E. Dobereiner and R. H. Crabtree, *Chemical Reviews*, 2010, **110**, 681-703.
9. K. Fujita, Z. Li, N. Ozeki and R. Yamaguchi, *Tetrahedron Lett*, 2003, **44**.
10. D. Pingen, C. Muller and D. Vogt, *Angew Chem Int Edit*, 2010, **49**, 8130-8133.
11. B. Gnanaprakasam, J. Zhang and D. Milstein, *Angew Chem Int Edit*, 2010, **49**, 1468-1471.
12. M. Hamid, C. L. Allen, G. W. Lamb, A. C. Maxwell, H. C. Maytum, A. J. A. Watson and J. M. J. Williams, *J Am Chem Soc*, 2009, **131**, 1766-1774.
13. N. Andrushko, V. Andrushko, P. Roose, K. Moonen and A. Borner, *Chemcatchem*, 2010, **2**, 640-643.
14. A. P. da Costa, M. Viciano, M. Sanau, S. Merino, J. Tejeda, E. Peris and B. Royo, *Organometallics*, 2008, **27**, 1305-1309.
15. D. Gnanamgari, E. L. O. Sauer, N. D. Schley, C. Butler, C. D. Incarvito and R. H. Crabtree, *Organometallics*, 2009, **28**, 321-325.
16. K. I. Fujita, Y. Enoki and R. Yamaguchi, *Tetrahedron*, 2008, **64**, 1943-1954.
17. Y. Z. Qiang Kang, *Green Chemistry*, 2012, **14**, 1016-1019.
18. G. Guillena, D. J. Ramon and M. Yus, *Chemical Reviews*, 2010, **110**, 1611-1641.
19. J. Xu, R. Zhuang, L. Bao, G. Tang and Y. Zhao, *Green Chemistry*, 2012, **14**, 2384-2387.
20. E. L. Zhang, H. W. Tian, S. D. Xu, X. C. Yu and Q. Xu, *Organic Letters*, 2013, **15**, 2704-2707.
21. G. Q. Zhang and S. K. Hanson, *Organic Letters*, 2013, **15**, 650-653.
22. Y. Nakajima, Y. Okamoto, Y. H. Chang and F. Ozawa, *Organometallics*, 2013, **32**, 2918-2925.
23. S. Musa, S. Fronton, L. Vaccaro and D. Gelman, *Organometallics*, 2013, **32**, 3069-3073.

Green Chemistry Accepted Manuscript

24. F. Cavani, F. Trifiro and A. Vaccari, *Catal Today*, 1991, **11**, 173-301.

25. D. Meloni, M. F. Sini, M. G. Cutrufello, R. Monaci, E. Rombi and I. Ferino, *J Therm Anal Calorim*, 2012, **108**, 783-791.

26. V. R. L. Constantino and T. J. Pinnavaia, *Inorganic Chemistry*, 1995, **34**, 883-892.

27. J. Kostal, A. Voutchkova-Kostal, B. Weeks, J. B. Zimmerman and P. T. Anastas, *Chemical Research in Toxicology*, 2012, **25**, 2780-2787.

28. A. Vaccari, *Applied Clay Science*, 1999, **14**, 161-198.

29. A. Vaccari, 1999, **- 14**, - 198.

30. J. S. Valente, F. Figueras, M. Gravelle, P. Kumbhar, J. López and J. P. Besse, *J. Catal.*, 2000, **189**, 370.

31. S. Velu and C. S. Swamy, *Appl Catal a-Gen*, 1997, **162**, 81-91.

32. L. Dussault, J. C. Dupin, E. Dumitriu, A. Auroux and C. Guimon, *Thermochim Acta*, 2005, **434**, 93-99.

33. S. Casenave, H. Martinez, C. Guimon, A. Auroux, V. Hulea, A. Cordoneanu and E. Dumitriu, *Thermochim Acta*, 2001, **379**, 85-93.

34. J. S. Valente, F. Figueras, M. Gravelle, P. Kumbhar, J. Lopez and J. P. Besse, *J Catal*, 2000, **189**, 370-381.

35. M. R. Othman, Z. Helwani, Martunus and W. J. N. Fernando, *Appl. Organomet. Chem.*, 2009, **23**, 335-346.

36. S. K. Yun and T. J. Pinnavaia, *Chem. Mat.*, 1995, **7**, 348-354.

37. S. K. Sharma, P. K. Kushwaha, V. K. Srivastava, S. D. Bhatt and R. V. Jasra, *Ind. Eng. Chem. Res.*, 2007, **46**, 4856-4865.

38. D. G. Evans and D. A. Xue, *Chemical Communications*, 2006, 485-496.

39. G. Fan, F. Li, D. G. Evans and X. Duan, *Chemical Society Reviews*, 2014, Advanced Article.

40. S. Nishimura, A. Takagaki and K. Ebitani, *Green Chemistry*, 2013, **15**, 2026-2042.

41. J. Perez-Ramirez, S. Abello and N. M. van der Pers, *Chem-Eur J*, 2007, **13**, 870-878.

42. K. K. Rao, M. Gravelle, J. S. Valente and F. Figueras, *J Catal*, 1998, **173**, 115-121.

43. D. P. Debecker, E. M. Gaigneaux and G. Busca, *Chem-Eur J*, 2009, **15**, 3920-3935.

44. S. Abello, F. Medina, D. Tichit, J. Perez-Ramirez, J. C. Groen, J. E. Sueiras, P. Salagre and Y. Cesteros, *Chem-Eur J*, 2005, **11**, 728-739.

45. M. J. Climent, A. Corma, S. Iborra and A. Velty, *J Catal*, 2004, **221**, 474-482.

46. A. R. Massah, R. J. Kalabashi, M. Toghiani, B. Hojati and M. Adibnejad, *E-Journal of Chemistry*, 2012, **9**, 2501-2508.

47. O. D. Pavel, B. Cojocaru, E. Angelescu and V. I. Parvulescu, *Appl Catal a-Gen*, 2011, **403**, 83-90.

48. D. G. Cantrell, L. J. Gillie, A. F. Lee and K. Wilson, *Appl Catal a-Gen*, 2005, **287**, 183-190.

49. V. H. Jadhav, D. K. Dumbre, V. B. Phapale, H. B. Borate and R. D. Wakharkar, *Catal Commun*, 2007, **8**, 65-68.

50. T. Baskaran, R. Kumaravel, J. Christopher and A. Sakthivel, *Rsc Advances*, 2014, **4**, 11188-11196.

51. B. M. Choudary, M. L. Kantam, A. Rahman, C. V. Reddy and K. K. Rao, *Angew Chem Int Edit*, 2001, **40**, 763-766.

52. K. Takehira and T. Shishido, *Catalysis Surveys from Asia*, 2007, **11**, 1-30.

53. V. K. Diez, C. R. Apesteguia and J. I. Di Cosimo, *J Catal*, 2003, **215**, 220-233.

54. P. R. Likhar, R. Arundhathi, M. L. Kantam and P. S. Prathima, *European Journal of Organic Chemistry*, 2009, 5383-5389.

55. K. Motokura, N. Hashimoto, T. Hara, T. Mitsudome, T. Mizugaki, K. Jitsukawa and K. Kaneda, *Green Chemistry*, 2011, **13**, 2416-2422.

56. S. Sueoka, T. Mitsudome, T. Mizugaki, K. Jitsukawa and K. Kaneda, *Chem Commun*, 2010, **46**, 8243-8245.

57. K. Motokura, D. Nishimura, K. Mori, T. Mizugaki, K. Ebitani and K. Kaneda, *J Am Chem Soc*, 2004, **126**, 5662-5663.

58. J. Bain, C. M. Munro, P. Cho and A. M. Voutchkova-Kostal, *New Journal of Chemistry*, 2012, **In preparation**.

59. B. M. Choudary, S. Madhi, N. S. Chowdari, M. L. Kantam and B. Sreedhar, *J Am Chem Soc*, 2002, **124**, 14127-14136.

60. W. H. Fang, Q. H. Zhang, J. Chen, W. P. Deng and Y. Wang, *Chem Commun*, 2010, **46**, 1547-1549.

61. T. Mitsudome, Y. Mikami, K. Ebata, T. Mizugaki, K. Jitsukawa and K. Kaneda, *Chem Commun*, 2008, 4804-4806.

62. T. Mitsudome, Y. Mikami, H. Funai, T. Mizugaki, K. Jitsukawa and K. Kaneda, *Angew Chem Int Edit*, 2008, **47**, 138-141.

63. K. Kaneda, T. Mitsudome, T. Mizugaki and K. Jitsukawa, *Molecules*, 2010, **15**, 8988-9007.

64. K. Takehira, T. Shishido, P. Wang, T. Kosaka and K. Takaki, *Physical Chemistry Chemical Physics*, 2003, **5**, 3801-3810.

65. J. Chen, Q. H. Zhang, W. H. Fang, Y. Wang and H. L. Wan, *Chinese J Catal*, 2010, **31**, 1061-1070.

66. W. H. Fang, J. S. Chen, Q. H. Zhang, W. P. Deng and Y. Wang, *Chem-Eur J*, 2011, **17**, 1247-1256.

67. R. K. Marella, C. K. P. Neeli, S. R. R. Kamaraju and D. R. Burri, *Catal Sci Technol*, 2012, **2**, 1833-1838.

68. R. J. Shi, F. Wang, X. L. Mu, N. Ta, Y. Li, X. M. Huang and W. J. Shen, *Chinese J Catal*, 2010, **31**, 626-630.

69. N. Kakiuchi, Y. Maeda, T. Nishimura and S. Uemura, *Journal of Organic Chemistry*, 2001, **66**, 6620-6625.

70. T. Nishimura, N. Kakiuchi, M. Inoue and S. Uemura, *Chem Commun*, 2000, 1245-1246.

71. R. Jenkins and R. L. Snyder, *Introduction to X-ray Powder Diffractometry*, John Wiley & Sons Inc., 1996.

72. S. Velu, V. Ramkumar, A. Narayanan and C. S. Swamy, *J Mater Sci*, 1997, **32**, 957-964.

73. T. Chen, F. Z. Zhang and Y. Zhu, *Catalysis Letters*, 2013, **143**, 206-218.

74. J. T. Feng, X. Y. Ma, Y. F. He, D. G. Evans and D. Q. Li, *Appl Catal a-Gen*, 2012, **413**, 10-20.

75. S. Narayanan and K. Krishna, *Appl Catal a-Gen*, 1998, **174**, 221-229.

76. D. E. Ramaker, J. de Graaf, J. A. R. van Veen and D. C. Koningsberger, *J Catal*, 2001, **203**, 7-17.

77. N. Kakiuchi, T. Nishimura, M. Inoue and S. Uemura, *Bulletin of the Chemical Society of Japan*, 2001, **74**, 165-172.

78. Granollers, M.; Brown, R.; An, N.; Yaseneva, Voutchkova-Kostal, A.; P.; Lapkin, A. Microcalorimetric studies of doped hydortalcite-like materials: effect of synthetic conditions. **Manuscript in preparation**